CVEL

THE CLEMSON UNIVERSITY VEHICULAR ELECTRONICS LABORATORY

TECHNICAL REPORT: CVEL-11-026

Mitigation of Unintentional Radiated Emissions from Tall VLSI Heatsinks Using Grounding Posts

Xinbo He and Dr. Todd Hubing
Clemson University

April 16, 2011

Table of Contents

Abstract

When a heatsink is mounted on an integrated circuit (IC) package above a printed circuit board (PCB) ground, noise from the IC can be coupled to it and radiate. At high frequencies, where the height of the heatsink is comparable to a quarter wavelength, the heatsink/board geometry can be an efficient antenna. One method to reduce heatsink radiation is to use shorting posts that bypass some of the noise current to the PCB. This report examines the effectiveness of shorting posts for reducing heatsink radiation.

1. Introduction

Since the introduction of very large scale integration (VLSI), the integration density and the operating frequency of integrated circuits have been increasing steadily. The huge number of semiconductor gates switching every second can draw significant amounts of current, which inevitably generates a lot of heat. Heatsinks are often used to carry this energy away and maintain an acceptable IC temperature. Heatsinks are generally made of copper, aluminum, and other metals that have high thermal conductivities; however, these metals also have high electrical conductivities. As IC operating frequencies increase, heatsinks are more likely to form resonant antennas with the power and ground planes on PCBs. This phenomenon is commonly observed in current VLSI applications [1, 2].

VLSI heatsinks can be modeled as a superposition of a patch antenna and a fat monopole [3]. When the heatsink height is small relative to its length and width, it radiates like a patch antenna. When the heatsink height is much larger than its length and width, it looks more like a monopole antenna [3, 4]. Different methods have been investigated to reduce the radiation from heatsinks [5, 6]. The damping of relatively short heatsinks is similar to the damping of chassis mounted circuits boards, which has been investigated in an earlier study [7].

One method to reduce the radiation from tall heatsinks is to use shorting posts that connect the heatsink body to the PCB ground [1, 2, 5, 8-10]. There can be one or more shorting posts and the locations of these posts can be anywhere around the heatsink. A general design guideline is that more posts work better [5]. However, design and cost constraints, limit the number of posts, thus it is important to understand how post positions and impedance affect the radiated emissions.

2. Calculation of Heatsink Driving Voltage

Fig. 1 shows an illustration of a tall heatsink mounted above an IC and its corresponding antenna model. Normally the PCB ground plane length and width are much larger than the heatsink cross section, and the heatsink can be modeled as a monopole or patch antenna [3]. A heatsink with a height much larger than its length and width can be modeled as a fat monopole antenna driven by the voltage coupled from the VLSI component. The radiation from fat monopole antennas has been well studied. Once the driving voltage is known, the radiated emissions can be readily obtained.

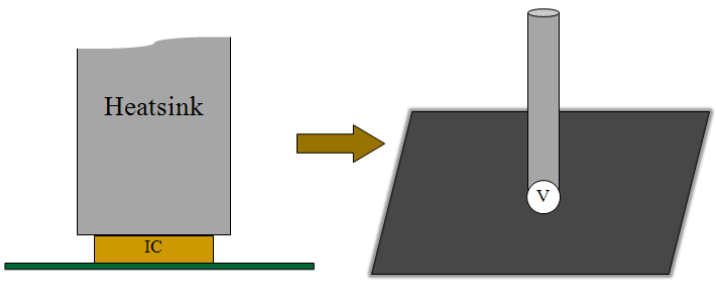

Fig. 1. A tall heatsink mounted on an IC above a PCB and its simplified model.

When conducting posts are mounted between the heatsink and the PCB ground, the voltage between the heatsink and the ground plane will be influenced by the size and location of the posts. Some of the source current will flow to the PCB ground through the posts and the rest will flow to the heatsink resulting in radiated emissions. The distribution of the noise current is shown in Fig. 2. To investigate how the posts reduce the heatsink radiation, it is necessary to determine the driving voltage of the heatsink, V_H.

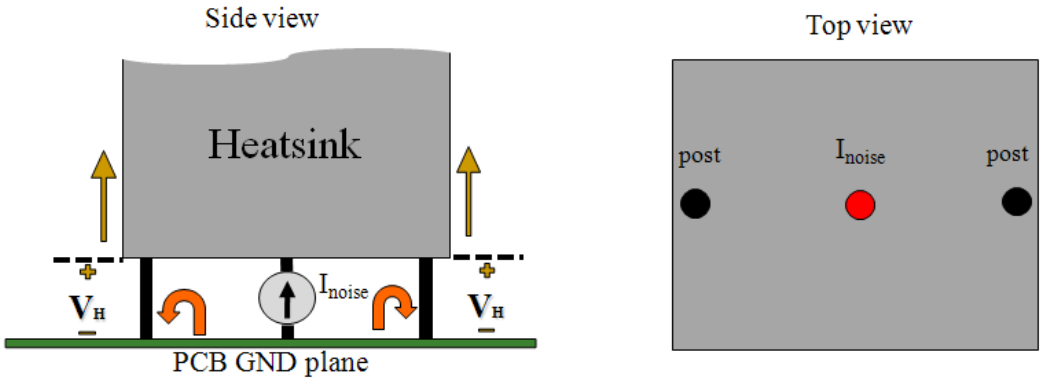

Fig. 2. Current distribution through the heatsink body and the mounted shorting posts.

At high frequencies, V_H is primarily due to the mutual inductance between the loop formed by the source current and the shorting posts and the "loop" formed by the monopole radiation. It is tempting to calculate the self inductance of the loop formed by the posts, the source, and the top and bottom plates of the cavity; then to multiply the impedance associated with this inductance by the current to get V_H. However, this approach is not correct. To illustrate this point, suppose the number of posts mounted along the edge of the patch is increased until the conducting posts form a "cage" around the enclosed noise source as shown in Fig. 3. In the limit as the number of posts approaches infinity, no current flows from the noise source to the external faces of the heatsink and consequently the heatsink does not radiate. The horizontal cross-section of the cavity now looks like a rectangular coaxial cable with the source as the inner conductor and the posts as the outer conductor. The inductance of this coaxial geometry is not zero; yet the voltage driving the monopole approaches zero.

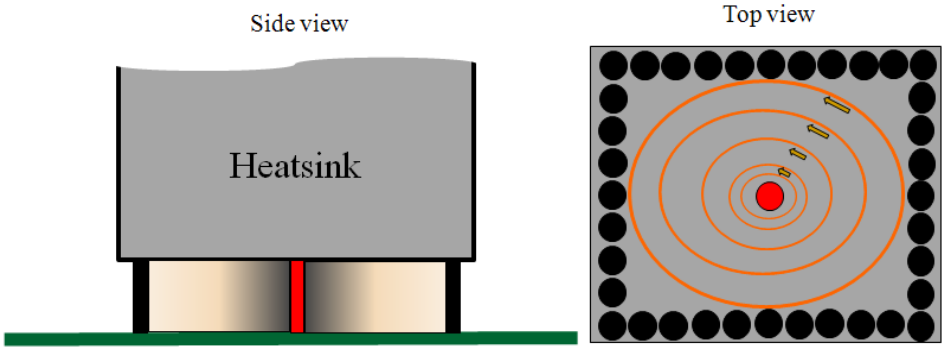

Fig. 3. Numerous posts that confine the field inside the cavity.

V_H is determined by the net magnetic flux that wraps the posts externally. Therefore, the mutual inductance between the source-post (inner) loop and the heatsink-post (outer) loop is the quantity of interest. Because the heatsink and circuit board geometries are very wide relative to the posts, little

magnetic flux wraps these portions of the loop. The total mutual inductance is therefore determined by the partial mutual inductances [12]between the source and the ground posts. Suppose there are two shorting posts and one noise source in the cavity as shown in Fig. 4. The net magnetic flux is determined by the partial mutual inductances between the source and the two ground posts [12-14].

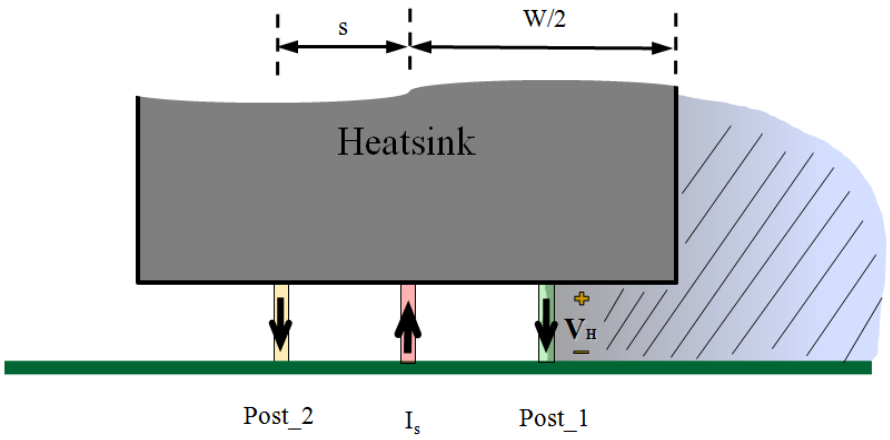

Fig. 4. Self and partial mutual inductance associated with one post (green).

The magnetic flux wrapping Post_1 externally is indicated by the shadowed area in Fig. 4. This flux is due to the current in Post_1 plus contributions from the currents in the source and Post_2. The voltage drop, V_H, can be determined by summing the contributions that each of these current segments makes to the total external magnetic flux.

For short posts between wide planes where all dimensions are short relative to a wavelength and displacement current can be neglected, the magnetic field intensity between the planes due to a post current I is [13][15]

$$\vec{H} = \frac{I}{2\pi r}\phi . \tag{1}$$

This is a reasonable approximation for the magnetic field between the heatsink and the PCB due to posts that are not too close to the edge of the heatsink. An expression for the magnetic field intensity in the shadowed region of Fig. 4 is more complicated, but can be represented as function of the distance from the outer post, r,

$$H = I \times f(r). \tag{2}$$

where $f(r)$ approaches zero as r approaches infinity at a rate exceeding $1/r$. The partial inductance can be calculated using the following formulas [13, 14].

$$L_{1s} = \frac{\mu_o h}{2\pi}\int_{s+a}^{W/2}\frac{1}{r}dr + \int_{W/2}^{\infty}\mu_o f(r)\,dA \tag{3a}$$

$$L_{11} = \frac{\mu_o h}{2\pi}\int_{a}^{W/2}\frac{1}{r}dr + \int_{W/2}^{\infty}\mu_o f(r)\,dA \tag{3b}$$

$$L_{12} = \frac{\mu_o h}{2\pi}\int_{2s+a}^{W/2}\frac{1}{r}dr + \int_{W/2}^{\infty}\mu_o f(r)\,dA . \tag{3c}$$

where L_{1s} is the mutual partial inductance between Post_1 and the source, L_{11} is the self partial inductance of Post_1, and L_{12} is the mutual partial inductance between Post_1 and Post_2. The width of the heatsink is W, the distance from the source to the posts is s, and the posts have a radius a and a height h.

The first terms in Eqs. (3a - c) can be evaluated explicitly. The resulting equations can be written as the sum of a calculable term and a constant that has the same value in all three equations,

$$L_{1s} = L_{1s}^{'} + L_o = \frac{\mu_o h}{2\pi} \ln \frac{W/2}{s+a} + \int_{W/2}^{\infty} \mu_o f(r)\, dA \tag{4a}$$

$$L_{11} = L_{11}^{'} + L_o = \frac{\mu_o h}{2\pi} \ln \frac{W/2}{a} + \int_{W/2}^{\infty} \mu_o f(r)\, dA \tag{4b}$$

$$L_{12} = L_{12}^{'} + L_o = \frac{\mu_o h}{2\pi} \ln \frac{W/2}{2s+a} + \int_{W/2}^{\infty} \mu_o f(r)\, dA\,. \tag{4c}$$

Summing the contributions from the partial and mutual inductances associated with Post_1, the voltage that drives the heatsink is given by

$$V_H = \omega I_1 L_{11} + \omega I_2 L_{12} - \omega I_s L_{1s}\,. \tag{5}$$

where I_s, I_1, and I_2 are the current flowing in the source, Post_1, and Post_2, respectively.

For symmetric configurations like the one in Fig. 4, the current flowing through each post is equal. For post impedances much smaller than the monopole radiation impedance, which is generally 36 Ω or greater, the total current flowing through all the posts is approximately equal to the source current. So, for this post configuration, we make the following approximation, $I_1 = I_2 = I_s/2$, and we rewrite (5) in terms of the source current,

$$\begin{aligned} V_H &= \omega I_s \left[\frac{L_{11} + L_{12}}{2} - L_{1s} \right] \\ &= \omega I_s \left[\frac{L_{11}^{'} + L_o + L_{12}^{'} + L_o}{2} - \left(L_{1s}^{'} + L_o \right) \right]. \\ &= \omega I_s \left[\frac{L_{11}^{'} + L_{12}^{'}}{2} - L_{1s}^{'} \right] \end{aligned} \tag{6}$$

In general, for a heatsink with n symmetrically located posts, the voltage driving the heatsink is given by,

$$V_H = \omega I_s \left[\frac{L_{11}^{'} + L_{12}^{'} + \bullet\bullet\bullet + L_{1n}^{'}}{n} - L_{1s}^{'} \right]. \tag{7}$$

Substituting the integrated terms in (4a) – (4c) for the corresponding terms in (6), and applying the properties of natural logarithms, (6) can be further simplified as

$$V_H = \omega I_s \left[\frac{L'_{11} + L'_{12}}{2} - L'_{1s} \right]$$
$$= \omega I_s \left[\frac{\frac{\mu_o h}{2\pi} \ln \frac{W/2}{a} + \frac{\mu_o h}{2\pi} \ln \frac{W/2}{2s+a}}{2} - \frac{\mu_o h}{2\pi} \ln \frac{W/2}{s+a} \right]. \quad (8)$$
$$= \frac{\omega I_s \mu_o h}{2\pi} \ln \frac{s+a}{\left[a(2s+a) \right]^{1/2}}$$

Similarly, (7) can be re-written as

$$V_H = \frac{\omega I_s \mu_o h}{2\pi} \ln \frac{s+a}{\left[a \times (s_2 + a) \times \cdots \times (s_n + a) \right]^{1/n}} \quad (9)$$

where s_i is the distance between Post_1 and Post_i.

The reduction in radiated emissions is equal to the reduction in V_H,

$$\text{Reduction} = \frac{|V_H|}{I_s \times R_{\text{heatsink}}} = \frac{\omega \mu_o h}{2\pi R_{\text{heatsink}}} \left| \ln \frac{s+a}{\left[a \times (s_2 + a) \times \cdots \times (s_n + a) \right]^{1/n}} \right| . \quad (10)$$

3. Validation of the Calculation Method

To validate the calculations in the previous section, PCB-heatsink geometries were simulated using full-wave electromagnetic modeling software [16]. The simulation results were then compared to results obtained using Eq. (10). In the first example, the heatsink dimensions are L_H = 45 mm, W = 45 mm, and H = 140 mm. The spacing between the heatsink and the PCB is 3 mm. A current source is located at the center of the cavity, with posts at the middle of the edges as shown in Fig. 5.

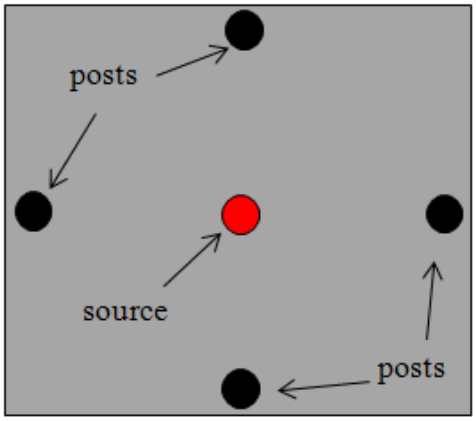

Fig. 5. Source and post locations viewed from the top of the heatsink cavity.

Five post combinations were evaluated with 1, 2, 3 or 4 posts. For the 2-post case, two possible locations were evaluated: two posts in the middle of opposite sides (180^o) or in the middle of adjacent sides (90^o). As a reference, the heatsink without any posts was also simulated. For each simulation, the magnitude of the maximum radiated electric field 3 meters away was obtained for frequencies up to 5 GHz as shown in Fig. 6.

In the full-wave simulations, the posts are simulated using a flat PEC ribbon instead of a round wire for convenience. The ribbon height is 3 mm and the width is 2 mm. For the purposes of the calculation in (8), the ribbon is equivalent to a circular cylindrical post of the same height with a radius equal to a quarter of the ribbon width [11].

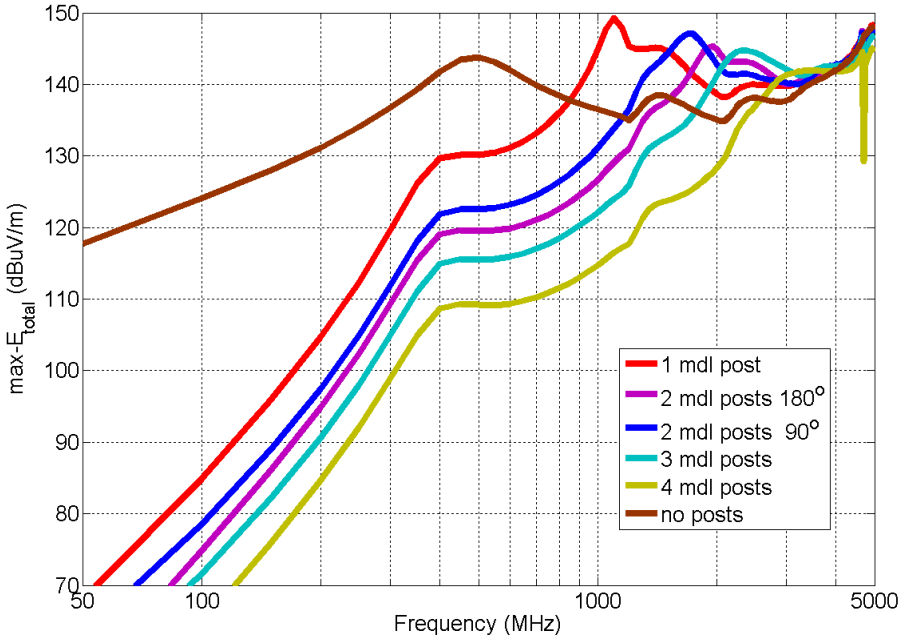

Fig. 6. Full-wave simulation results: maximum electric field vs. frequency.

In Fig. 6, the brown line represents the maximum radiated field from the heatsink without any posts. The peak at about 500 MHz is due to a resonance of the heatsink body. The heatsink height is much larger than its length and width. Thus it resonates like a monopole at low frequencies. The resonant frequency is approximately

$$f = \frac{300}{\lambda} \approx \frac{300}{4(H+h)/0.96} = \frac{300}{4(0.14+0.003)/0.96} \approx 500 \text{ MHz} \ , \qquad (11)$$

where H is the height of the heatsink, and the factor 0.96 is applied to take into account the thickness of the monopole [11].

With shorting posts, the radiated field at frequencies at or below the first monopole resonance is decreased. As more posts are added, the radiated fields are reduced and the effective frequency range is extended. In the two-post case, the 180^o configuration results in better reduction than the 90^o case. This is due to the lower partial mutual inductance in the 180^o configuration.

For each post configuration, the radiation reduction at the first monopole resonance was also calculated using the partial inductance method, Eqs. (1) - (10). The calculated reduction from the full-wave simulation and the partial inductance calculation are listed in Table 1. Note that the 2-90^o configuration and the 3-post configuration are not symmetric and therefore violate one of assumptions made when deriving (10). Nevertheless, for all 5 of the post configurations, the difference between the full-wave calculations and results obtained using Eqs. (1) – (10) are less than 2 dB.

Table 1. Radiation reduction for different post configurations

Configuration of Posts	Full-wave (dB)	Partial L (dB)
1	12.1	13.6
2 – 90°	19.9	21.6
2 - 180°	22.7	22.7
3	26.9	27.2
4	33.1	31.6

The radiated emissions with 2 posts on opposite sides of the heatsink are about 10 dB lower than the emissions with 1 post. If the reduction were simply a function of post impedance (self partial inductance), one might expect the reduction to be 6 dB (a factor of 2). This emphasizes the importance of evaluating the partial mutual inductances of the shorting post configuration, and placing the posts in positions that maximize the cancelling of magnetic flux outside the PCB-heatsink cavity.

4. LC Resonance Damping

In the previous section, it was shown that shorting posts can help to reduce tall heatsink radiation at frequencies up to and including the first monopole resonance. However, (in Fig. 6) LC resonances occurring at frequencies higher than the first monopole resonance resulted in increased radiation at those frequencies. The L in these resonances comes from the inductance associated with the posts and C from the top and bottom surfaces of the 2D cavity. At resonance, peaks occur in the voltage, V_H, that drives the monopole. Adding more posts reduces the inductance and causes the LC resonance to occur at higher frequencies.

It is often desirable to damp these LC resonances, while maintaining the low-frequency radiation reductions. One method of damping is to introduce lossy components in series within the shorting posts. These lossy components reduce the resonance quality factor. With a resistor mounted in series with the post's connection to the ground plane, the equivalent circuit for the LC resonance is replaced with C parallel to $R+j\omega L$. The quality factor of such an RLC circuit is

$$Q = \frac{1}{R}\sqrt{\frac{L}{C}} \ . \tag{12}$$

To validate the effectiveness of a lossy component in series with the shorting posts, a heatsink of the same size as that used in Fig. 5 with two posts (180^o configuration) was analyzed. In this case the posts were wider, equivalent to a radius of 1.25 mm, than those used in Fig. 5 and seven simulations were done with variable resistance in the posts. In each case, the resistors in the two posts had the same value. The maximum radiated electric field at 3 meters obtained from these simulations is plotted in Fig. 7.

As shown in Fig. 7, the LC resonance peaks are reduced by adding resistance in series with the two posts. The higher the resistance value, the more the peak is damped. At low frequencies, where the impedance of the posts is dominated by the resistance, the radiation increases. There is a trade-off between the squelching of the low frequency radiation and the damping of the LC resonance. It is apparent from Fig. 7 that as the resistance of the posts increases above a certain value, the LC resonance is well damped and cannot be reduced further.

Forcing the RLC circuit to be critically damped (Q = 0.5), an optimal value of R is obtained. For the heatsink in this example, the effective inductance associated with the posts is 0.53 nH and the patch capacitance is 7.7 pF. Thus the optimal R is approximately 16 Ω. In Fig. 7, this value falls between the 10-Ω and 37-Ω simulations, where the LC resonance appears to be well damped. A lower resistance

does not damp the LC resonance enough, while a higher value sacrifices the low frequency radiation reduction.

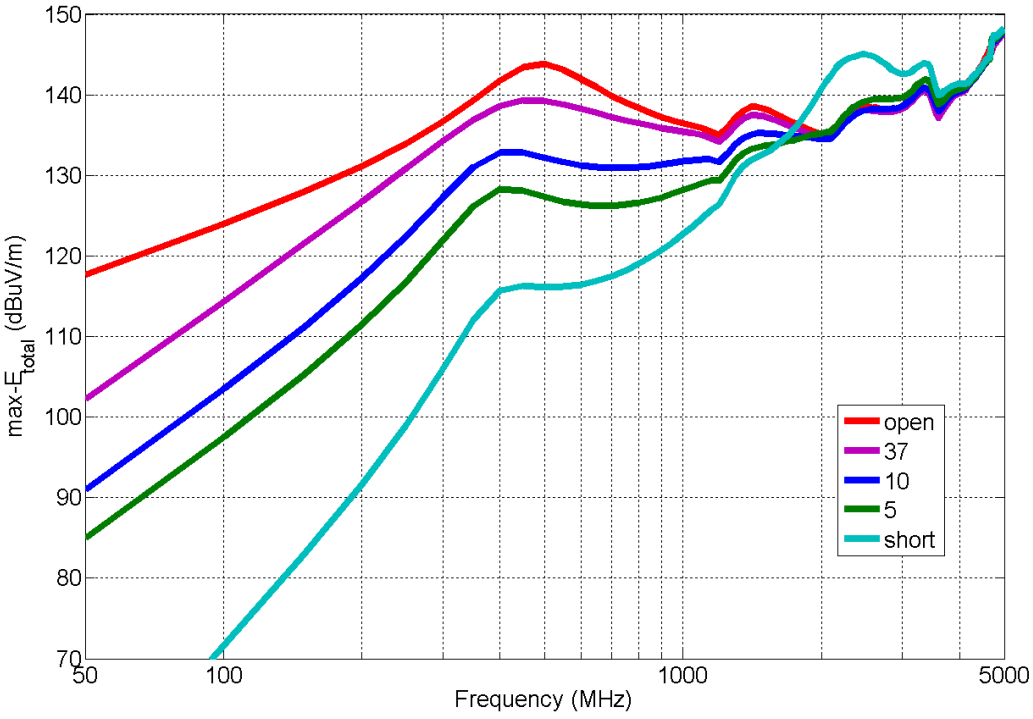

Fig. 7. Effect of damping the *LC* resonance with different resistances in series with the shorting posts.

The reduction in field strength at the first heatsink resonance for various post resistances is shown in Table 2.

Table 2. Radiation reduction at first heatsink resonance

Series R in post (Ω)	Full-wave (dB)	Partial L (dB)
37	4.5	6.5
10	11.6	13.2
5	16.5	17.7
0	27.7	26.5

It is also worth noting that the squelching effect is about 5 dB better for the shorting posts (0 Ω resistance) in Table 2 than the 0 Ω post configuration in Table 1. The only difference between the two models is wider posts. Wider posts have lower partial inductances and work better to reduce the low frequency radiation.

In these simulations, loss associated with the source was neglected. It is also important to note that the LC resonances occurred at frequencies that may be above the highest frequency of concern in a given application. For these reasons, it may not always be necessary or desirable to damp LC resonances with a series resistance. In some situations it may be optimal to add resistance to some, but not all shorting posts. This option for damping PCB chassis resonances was explored in [7].

5. Summary

In this report, the use of shorting posts to reduce heatsink radiation was examined. The effectiveness of shorting posts can be analyzed using the concepts of partial inductance and partial mutual inductance, with Eqs. (1) – (10). Using the partial inductance calculations described in this report, the effectiveness of shorting posts can be predicted; therefore this technique can be used to optimize the design and placement of these posts. The method was validated using full-wave electromagnetic models of heatsinks over ground planes. The full-wave and partial inductance models calculate reductions in the amplitude of the first monopole resonance that are within 2 dB of each other for all 5 post configurations.

The report also describes a procedure for damping the LC resonance caused by shorting posts. Adding resistance in series with the posts reduces the quality factor of the equivalent circuit. By forcing the RLC circuit to be critically damped, an optimal R can be calculated using Eq. (12), where L can be obtained with Eqs. (1) – (10) and C is approximated using the parallel plate capacitance formula.

References

[1] C.F. Lee, K. Li, S.Y. Poht, R.T. Shin, and J.A. Kong, "Electromagnetic radiation from a VLSI package and heatsink configuration," *Proc. 1991 IEEE Int. Symp. Electromagn. Compat.*, pp. 393-398, Aug. 1991.

[2] K. Li, C. F. Lee, S. Y. Poh, R. T. Shin, and J. A. Kong, "Application of FDTD method to analysis of electromagnetic radiation from VLSI heatsink configurations," *IEEE Trans. Electromagn. Compat.*, vol. 35, no. 2, pp. 204–214, 1993.

[3] X. He, and T. Hubing, "A closed-form expression for estimating heatsink maximum radiated emissions," *Clemson Vehicular Electronics Laboratory Technical Report: CVEL-11-025*.

[4] D. Hockanson and R. D. Slone, "Investigation of EMI coupling at CPU interconnect," *Proc. 2004 IEEE Int. Symp. Electromagn. Compat.*, vol. 2, pp. 424–429, August 2004.

[5] Bruce Archambeault, Juan Chen, Satich Pratepeni, Lauren Zhang, David Wittwer, "Comparison of Various Numerical Modeling Tools Against a Standard Problem Concerning Heat Sink Emissions - Standard Modeling Paper 3," IEEE EMC Society TC 9 website, http://www.ewh.ieee.org/cmte/tc9/

[6] J. C. Diepenbrock, B. Archambeault, L.D. Hobgood, "Improved grounding method for heat sinks of high speed processors," *Proc. Electronic Components and Technology Conference*, vol. 51, pp. 993-996, 2001.

[7] X. He, T. Hubing, H. Ke, N. Kobayashi, K. Morishita and T. Harada, "Calculation of optimal ground post resistance for reducing emissions from chassis-mounted printed circuit boards," *IEEE Trans. on Electromagn. Compat.*, accepted, August 2010.

[8] C. E. Brench, "Heatsink radiation as a function of geometry," *Proc. 1994 IEEE Int. Symp. Electromagn. Compat.*, pp. 105–109, 1994.

[9] J. F. Dawson, A. C. Marvin, A. Nothofer, J. E.Will, and S. Hopkins, "The effects of grounding on radiated emissions from heatsinks," *Proc. 2001 IEEE Int. Symp. Electromagn. Compat.*, pp. 1248–1252, Aug. 2001.

[10] C. Wang, J. L. Drewniak, J. L. Knighten, D. Wang, R. Alexander, and D. M. Hockanson, "Grounding of heatpipe/heatspreader and heatsink structures for EMI mitigation," *Proc. 2001 IEEE Int. Symp. Electromagn. Compat.*, vol. 2, pp. 916 – 920, 2001.

[11] C. A. Balanis, *Antennas, 3rd Edition*, Wiley-Interscience, Apr. 2005.

[12] A. Ruehli, "Inductance calculations in a complex integrated circuit environment," *IBM J. Res. Dev.*, no. 5, pp. 470–481, Sept. 1972.

[13] T. H. Hubing, T. P. Van Doren, and J. L. Drewniak, "Identifying and quantifying printed circuit board inductance," *Proc. IEEE Int. Symp. Electromagn. Compat.*, Chicago, IL, pp. 205–208, Aug.1994.

[14] C.R. Paul, *Inductance: Loop and Partial*, John Wiley, Hoboken, N.J., 2010.

[15] H. Johnson, M. Graham, *High Speed Signal Propagation: Advanced Black Magic*, pp. 354-358, Prentice Hall Mar. 6, 2003.

[16] Y. Ji and T. Hubing, "EMAP5: A 3D hybrid FEM/MOM code," *Journal of the Applied Computational Electromagnetics Society*, vol. 15, no. 1, Mar. 2000, pp. 1-12.